Chemical Engineering Journal 164 (2010) 238–245

Contents lists available at ScienceDirect

Chemical Engineering Journal

journal homepage: www.elsevier.com/locate/cej

Trend prediction in velocity distribution among microchannels based on the analysis of frictional resistances

Minqiang Pan[a,*], XiaoLing Wei[a], Dehuai Zeng[b], Yong Tang[a,b]

[a] Key Laboratory of Surface Functional Structure Manufacturing of Guangdong Higher Education Institutes, South China University of Technology, Guangzhou 510640, China
[b] School of Mechatronics and Control Engineering, Shenzhen University, Shenzhen 518060, China

ARTICLE INFO

Article history:
Received 20 May 2010
Received in revised form 10 August 2010
Accepted 10 August 2010

Keywords:
Microchannel array
Velocity distribution
Frictional resistance
Resistance network

ABSTRACT

Velocity distribution among microchannel plays an important role in the performances of microchannel reactors. The optimization of structural parameters by enabling narrow uniform velocity distribution among microchannels is regarded as one of the effective design methods. On the basis of the previously developed model, the effects of structural parameters on the velocity distribution are studied and the relationship between frictional resistances and pressure drop are investigated in this work. It is found that the variation of pressure drop distribution among microchannels due to the variation of frictional resistances is the underlying reason for the variation of velocity distribution among microchannels. Compared with the manifold structural parameters, the microchannel structural parameters show more influence on the velocity distribution. High-aspect-ratio microchannels are in favor of obtaining relatively uniform velocity distribution. By the combination of the calculation of frictional resistances with descriptive geometry, it can predict the trend of velocity distribution among microchannels with the variation of structural parameters without applying complicated theoretical model or numerical simulation.

1. Introduction

Microchannel reactors have several advantages compared with traditional reactors, such as high heat and mass transfer efficiency, light weight and compactness, and hence have the widespread application prospect in portable power devices. Laminated-sheet structure is one of the fundamental constructions for microchannel reactors, in which multiple microchannel sheets with manifold structures are stacked together to form a reaction unit [1–3], as shown in Fig. 1. Microchannel structure plays an important role on the performances of laminated-sheet microchannel reactors. Since relatively uniform velocity distribution among microchannels offers clear advantages such as uniform residence time distribution among microchannels, high conversion rate and selectivity of process, the optimization of microchannel structural parameters by obtaining relatively uniform velocity distribution among microchannels is regarded as one of the effective design methods.

A majority of researches [4–6] had been focused on the optimization of microchannel structure by analyzing the fluid velocity distribution among microchannels assisted by theoretical modeling or numerical simulation. Commenge et al. [4] developed an approximate pressure drop model to optimize the velocity and residence time distribution among microchannels. The linear relation of pressure drop and velocity between microchannels was established, and then a rapid calculation method of fluid velocities in the microchannels was proposed. The calculation results were validated against finite-volume simulations. Amador et al. [5] applied an electrical resistance network model to analyze the flow distribution among microchannels with consecutive and bifurcation manifold structures. Two methods were proposed to achieve uniform flow distribution in the consecutive structure, one was by minimizing pressure drop in the distributing/collecting channels and the other was by equalizing pressure drop in the reaction channels. Tonomura et al. [6] investigated the flow uniformity among branched microchannels with rectangular manifolds by CFD simulation and proposed an automatic shape optimization method for the design of plate-fin microdevices. Delsman et al. [7] studied nine different plate geometries at flow rates between 0.1 and 100 ms^{-1} by a three-dimensional CFD model to optimize the flow distribution. Simulation results showed that the inertia effects started to affect the flow distribution when the velocity surpassed a certain value.

In our previous work [8], we proposed a theoretical model to study the characteristics of velocity distribution among microchannels with triangle manifolds. A simplified method was developed by dividing the manifolds into multiple approximate rectangular channels based on the pressure distribution simulated by Fluent™.

* Corresponding author. Tel.: +86 20 8711 4634; fax: +86 20 8711 4634.
E-mail address: mqpan@scut.edu.cn (M. Pan).

1385-8947/$ – see front matter © 2010 Elsevier B.V. All rights reserved.
doi:10.1016/j.cej.2010.08.024

Nomenclature

D_H	hydraulic nominal diameter (m)
E	channel depth (m)
H_{in}	side length of inlet manifold (m)
i, j	integer variable
K_R	the ratio of change amplitude of R_{fc} to R_{fi} (m)
L	channel length/segment length (m)
L_{in}	length of approximate rectangular channel (m)
L_m	bottom length of manifold (m)
max	maximum value
min	minimum value
N	microchannel number
ΔP	pressure drop (Pa)
$\Delta P_{fc}(j)$	frictional pressure drop in the jth microchannel (Pa)
$\Delta P_{fi}(j)$	frictional pressure drop in the jth approximate rectangular channel of the inlet manifold (Pa)
$\Delta P_{fo}(j)$	frictional pressure drop in the jth approximate rectangular channel of the outlet manifold (Pa)
ΔP_T	overall pressure drop (Pa)
R_f	frictional resistance (Pa s m^{-3})
$R_{fc}(j)$	frictional resistance in the jth microchannel (Pa s m^{-3})
$R_{fi}(j)$	frictional resistance in the jth approximate rectangular channel of the inlet manifold (Pa s m^{-3})
R_{fi} (m)	average value of frictional resistances in the approximate rectangular channels of the inlet manifold (Pa s m^{-3})
$R_{fo}(j)$	frictional resistance in the jth approximate rectangular channel of the outlet manifold (Pa s m^{-3})
R_{pi}	radius of the inlet (m)
U	fluid velocity (ms^{-1})
$U_c(j)$	the velocity value in each microchannel (ms^{-1})
U_m	average velocity of microchannels (ms^{-1})
U_T	entrance velocity of the simplified resistance network model (ms^{-1})
W	channel width (m)
X_{pi}	horizontal coordinate of the inlet center related to point C_1 (m)
Y_{pi}	vertical coordinate of the inlet center related to point C_1 (m)

Subscripts

c	microchannel
in, i	inlet manifold
out, o	outlet manifold

Greek letters

λ_{NC}	non-circular coefficient
μ	viscosity (Pa s)
$\Delta\gamma\%$	estimated parameters of pressure distribution among microchannels
$\gamma(j)$	the ratio of pressure drop caused by frictional loss in any microchannel j to the overall pressure drop
γ_m	average value of $\gamma(j)$ of all the microchannels
$\sigma_U\%$	estimated parameters of velocity distribution

And the relationship between the velocities and pressure drops in microchannels and approximate rectangular channels were established by an equivalent simplified resistance network model. Then the effects of singular losses on the velocity distributions were analyzed. On the basis of the previously developed model, the effects of structural parameters of microchannel and manifold on the velocity distribution are firstly studied in this work, and the relationship between the pressure drop and velocity distribution are analyzed. Then the underlying reason for the variation of velocity distribution is investigated by analyzing the variation of frictional resistances of microchannels or approximate rectangular channels. By combining the calculation of frictional resistances with descriptive geometry, it could predict the trend of velocity distribution among microchannels with the variation of structural parameters. When the structural parameters of microchannel or manifold are changed, the method can be used to predict the trend of velocity distribution among microchannels without applying complicated theoretical model or numerical simulation.

2. Microchannel array model

2.1. Division of manifolds

In the laminated-sheet structure, each sheet consists of an inlet and corresponding manifold, an outlet and corresponding manifold as well as parallel microchannels with rectangular or semicircular cross-sections in general, as shown in Fig. 2(a). The direction of fluid is perpendicular to the inlet and outlet. In the previous research [8], the flow zone of fluid was extracted from the microchannel sheet as a research object, as shown in Fig. 2(b). And then the manifolds were divided into two parts by the segment C_1F_1 which was perpendicular to the bisector SP_i of $\angle GSC_1$, one was the polygon $T_1T_2C_1F_1$ as transition chamber, the other was the polygon $C_1C_{N+1}GF_1$ as connected chamber. The former showed little effects on the velocity distribution and the latter was further divided into multiple approximate rectangular channels $C_iC_{i+1}F_{i+1}F_i$ ($i = 1, 2, \ldots, N$) with same length L_{in}, as shown in Fig. 2(c). The segment C_iF_i($i = 1, 2, \ldots,$ N) as the inlet of each approximate rectangular channel was perpendicular to SP_i. The length L_{in} of each approximate rectangular channel could be calculated as follows:

$$L_{in} = \frac{L_m \sin \angle F_iC_iC_{N+1}}{N} \tag{1}$$

where L_m represented the bottom length C_1C_{N+1} of manifold.

2.2. Relation model between pressure drop and frictional resistance

According to Hagen–Poiseuille equation, for a laminar flow in rectangular channels, the pressure drop ΔP due to frictional losses is defined as:

$$\Delta P = \frac{32\,\mu L\,\lambda_{NC}}{D_H^2} U = R_f U \tag{2}$$

where, D_H and λ_{NC} are the hydraulic nominal diameter and non-circular coefficient [4,5], respectively. R_f is referred to frictional resistance and can be obtained as follows [8]:

$$R_f = \frac{12\,\mu L}{\min^2(W,E)\left(1 - 0.351\ \min\left((E/W),(W/E)\right)\right)^2} \tag{3}$$

Here, W and E represent the channel width and depth, respectively.

Eq. (2) indicates the pressure drop and velocity are linearly dependent without considering the singular losses. After the definition of frictional resistance, the microchannel array model can be simplified to a relation model between pressure drop and frictional resistance, as shown in Fig. 3. In this model, the frictional resistances in the microchannels, the approximate rectangular channels of the inlet and outlet manifold are represented as electrical resistances $R_{fc}(j)$, $R_{fi}(j)$ and $R_{fo}(j)$($j = 1, 2, \ldots, N$), respectively. The pressure drops caused by singular losses are much smaller than that caused by frictional losses under low Reynolds numbers and in hence they are neglected here.

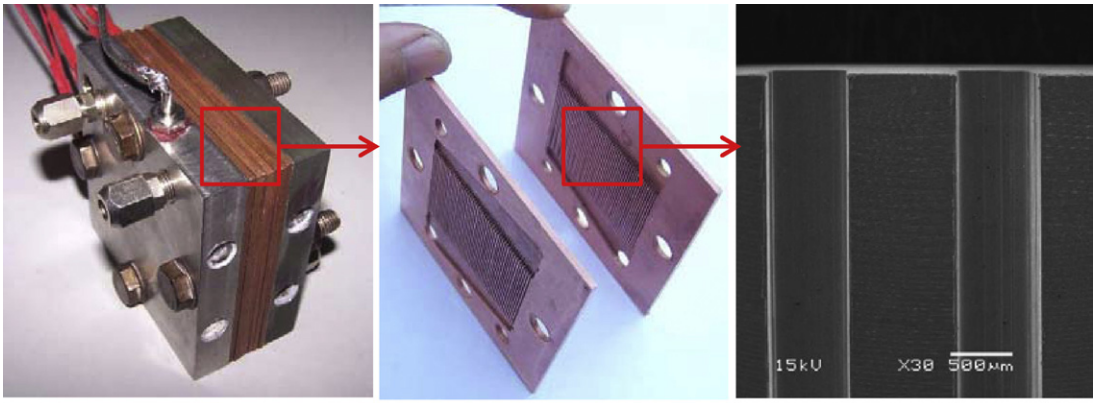

Fig. 1. Laminated-sheet structure.

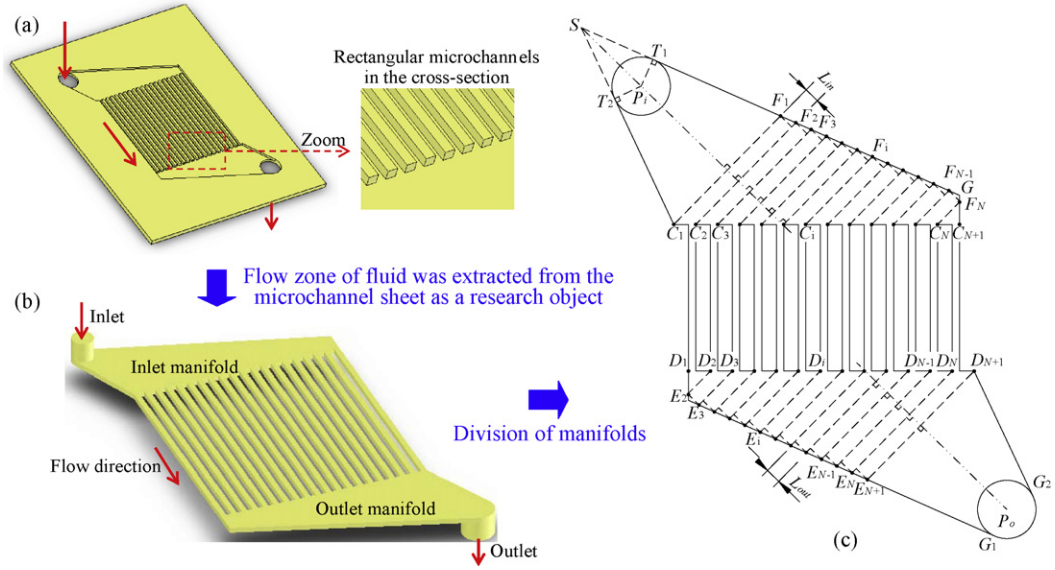

Fig. 2. Microchannel array and the division method of manifolds.

Eq. (3) shows that the frictional resistance R_f of each channel is invariant when all the structural parameters of microchannels or approximate rectangular channels are given. Therefore, the variation of velocity value in a single microchannel is resulted from the variation of the pressure drop, as indicated in Eq. (2). The differences of pressure drop distribution among microchannels could be the possible reasons resulted in the variation of velocity distribution among microchannels. The objective of the present work is to study the effects of structural parameters on the velocity distribution among microchannels based on a special case illustrated in Table 1, and further analyze the relationships between the pressure drop and velocity distribution. Then the variations of frictional resistances are analyzed on the basis of Eq. (3) and descriptive geometry to analyze the reason for the variation of pressure drop and velocity distribution if any structural parameter was changed.

Here the rectangular microchannel array model with triangle manifolds [8] is adopted and the inlet manifold and outlet manifold are centrosymmetric. The structural parameters of outlet manifold

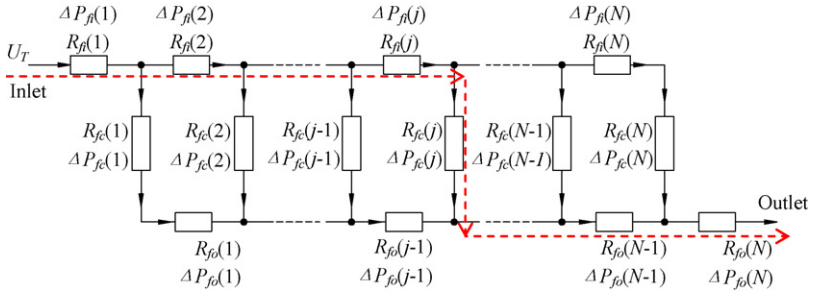

Fig. 3. Relation model between pressure drop and frictional resistance.

Table 1
Structural parameters of microchannel array model.

Microchannel structural parameters	Microchannel number N	20
	Microchannel length L_c	20 mm
	Microchannel width W_c	500 μm
	Microchannel depth E	500 μm
Inlet manifold structural parameters	Side length GC_{N+1} of manifold H_{in}	2 mm
	Bottom length $C1C_{N+1}$ of manifold L_m	20 mm
	The coordinate of inlet center P_i related to point $C_1(X_{pi}, Y_{pi})$	(−2 mm, 7 mm)
	Inlet radius R_{pi}	2 mm

can be easily obtained from that of the inlet manifold shown in Table 1. The liquid water at normal temperature and pressure is selected as the fluid and the entrance velocity is preset to 1 mm s^{-1}. Although the study is based on a single case, the results can be used to improve the design process of structural parameters of a microchannel sheet in general.

2.3. Estimated parameters

In this work, the velocity and pressure drop distribution are quantitatively estimated by the parameters of σ_U% and $\Delta\gamma$%, respectively. They are defined as below and calculated by the previously established model of velocity distribution among microchannels with triangle manifolds. The principle of calculation can be referred to Ref. [8].

$$\sigma_U\% = 100\sqrt{\frac{1}{N}\sum_{i=1}^{N}\left(\frac{U_c(i)}{U_m}-1\right)^2} \quad (i = 1,\ 2,\ \ldots,\ N) \tag{4}$$

where, $U_c(i)$ represents the velocity value in each microchannel, U_m is the average value of all microchannel velocities, as defined below:

$$U_m = \frac{1}{N}\sum_{i=1}^{N}U_c(i) \quad (i = 1,\ 2,\ \ldots,\ N) \tag{5}$$

$$\Delta\gamma\% = 100\frac{\max[\gamma(j)] - \min[\gamma(j)]}{\gamma_m} \quad (j = 1,\ 2,\ \ldots,\ N) \tag{6}$$

where $\gamma(j)$ represents the ratio of pressure drop caused by frictional loss in any microchannel j to the overall pressure drop, as defined below. Max $[\gamma(j)]$ and min $[\gamma(j)]$ are the maximum and minimum value of $\gamma(j)$, respectively.

$$\gamma(j) = \frac{\Delta P_c(j)}{\Delta P_T} \quad (j = 1, 2, \ldots, N) \tag{7}$$

γ_m is the average value of $\gamma(j)$ of all the microchannels, as defined below:

$$\gamma_m = \frac{1}{N}\sum_{j=1}^{N}\gamma(j) \quad (j = 1,\ 2,\ \ldots,\ N) \tag{8}$$

The overall pressure drop can be calculated as below by the route from the inlet to outlet via any microchannel j, as the dotted line depicted in Fig. 3.

$$\Delta P_T = \sum_{i=1}^{j}\Delta P_{fi}(i) + \Delta P_{fc}(j) + \sum_{i=j}^{N}\Delta P_{fo}(i) \quad (j = 1, 2, \ldots \text{ or } N) \tag{9}$$

Here $\sum_{i=1}^{j}\Delta P_{fi}(i)$ is the sum of pressure drops caused by frictional losses from the 1st to jth approximate rectangular channels of the inlet manifold. And $\sum_{i=j}^{N}\Delta P_{fo}(i)$ is the sum of pressure drops caused by frictional losses from the jth to Nth approximate rectangular channels of the outlet manifold.

Obviously, smaller σ_U% and $\Delta\gamma$% suggest more uniform distribution of velocities and pressure drops among microchannels, respectively.

3. Results and discussion

3.1. Effects of independent variation of microchannel structural parameters

Table 2 presents the influences of independent variation of microchannel structural parameters on the velocity and pressure drop distribution. It could be found that the value of γ_m was increased with increasing L_c and E, but decreased with increasing W_c. On the other hand, the values of $\Delta\gamma$% and σ_U% had the same trend with the variation of microchannel structural parameters. They were both decreased with increasing L_c and E, but increased with increasing W_c, which indicated that the velocity and pressure drop distribution became more uniform with larger L_c, E or smaller W_c. However, how the microchannel structural parameters affected the variation of γ_m, $\Delta\gamma$% and σ_U% was unknown yet, and their relationship was investigated by the analysis of the variation of frictional resistances as follows.

3.1.1. The variation of L_c

According to Eq. (3), the value of R_{fc} increased with the increasing L_c when W_c and E remained unchanged. The increase of R_{fc} could result in the increase of $\gamma(j)$ and corresponding increase of γ_m based on Eqs. (2), (7) and (8). As a result, the differences $\Delta\gamma$% of pressure drop among microchannels decreased due to the increase of average pressure drops in microchannels. According to Eq. (2), the pressure drops due to frictional losses were the intrinsic reason for the variation of velocity, and hence the value of σ_U% could decrease with the decreasing $\Delta\gamma$%. Therefore the velocity distribution among microchannels became more uniform with increasing L_c.

3.1.2. The variation of W_c

According to Eq. (3), the variation of R_{fc} with the variation of W_c was considered in two aspects as follows, when $W_c \le E$ and $W_c > E$.

(1) When $W_c \le E$

The following equation could be obtained from Eq. (3) when $W_c \le E$.

$$R_{fc} = \frac{12\ \mu L_c}{W_c^2(1 - 0.351(W_c/E))^2} \tag{10}$$

Then the denominator of Eq. (10) was defined as a function of W_c and its derivative could be obtained from Eq. (12):

$$f(W_c) = W_c^2\left(1 - 0.351\frac{W_c}{E}\right)^2 \tag{11}$$

$$f'(W_c) = 2W_c\left(1 - 0.351\frac{W_c}{E}\right)\left(1 - 0.702\frac{W_c}{E}\right) \tag{12}$$

Let $f'(W_c)$ equal to 0, four monotone intervals of the curve of $f(W_c)$ could be worked out, that was, $[0, (E/0.702)]$ and $[(E/0.351), +\infty)$ as the monotone increasing intervals while $(-\infty, 0]$ and $[(E/0.702), (E/0.351)]$ as the monotone decreasing intervals. Since

Table 2
Effects of microchannel structural parameters on the values of γ_m, $\Delta\gamma\%$ and $\sigma_U\%$.

L_c (mm)	10	20	30	40	50
γ_m	0.564	0.721	0.795	0.838	0.866
$\Delta\gamma\%$	12.935	6.710	4.531	3.421	2.747
$\sigma_U\%$	4.043	2.097	1.416	1.068	0.858
W_c(μm)	100	200	300	400	500
γ_m	0.991	0.954	0.886	0.803	0.721
$\Delta\gamma\%$	0.544	1.267	2.621	4.525	6.710
$\sigma_U\%$	0.169	0.359	0.742	1.354	2.097
E(μm)	100	200	300	400	500
γ_m	0.576	0.609	0.645	0.682	0.721
$\Delta\gamma\%$	12.839	11.182	9.602	8.108	6.710
$\sigma_U\%$	4.119	3.563	3.039	2.550	2.097

W_c belonged to the range of [0, (E/0.702)] when $W_c \le E$, the value of $f(W_c)$ increased with the increasing W_c. As a result, R_{fc} decreased with the increasing W_c according to Eq. (10).

(2) When $W_c > E$

When $W_c > E$, Eq. (3) could be changed to Eq. (13) as follows:

$$R_{fc} = \frac{12\,\mu L_c}{E^2(1-0.351(E/W_c))^2} \tag{13}$$

Obviously, R_{fc} decreased with the increasing W_c.

From the above analyses, R_{fc} decreased with the increasing W_c, regardless of whether it was on the condition of $W_c \le E$ or $W_c > E$. The decrease of R_{fc} indicated that the pressure drop in microchannels lost the dominant position in the overall pressure drop. And hence γ_m decreased and $\Delta\gamma\%$ increased, which led to the increase of $\sigma_U\%$ from 0.169 to 2.097 when W_c increased from 100 to 500 μm.

3.1.3. The variation of E

It could be inferred that R_{fc} decreased with increasing E due to the symmetry of W_c and E in the Eq. (3). However, the variations of γ_m, $\Delta\gamma\%$ and $\sigma_U\%$ with the variation of E were opposite to those with the variation of W_c. As shown in Table 2, γ_m increased as well as $\Delta\gamma\%$ and $\sigma_U\%$ decreased with the increasing E. Unlike the variation of W_c, the increase of E also resulted to a corresponding increase of the depth of inlet and outlet manifold. And the frictional resistances of approximate rectangular channels of manifolds also decreased with the increasing E. The possible reason responsible for the increase of γ_m lay in that the reduced pressure drop due to the decrease of frictional resistances in the manifolds was smaller than that in the microchannels. As a result, the ratio of pressure drop in microchannels to the overall pressure drop increased and led to a corresponding decrease of $\Delta\gamma\%$. Therefore, the velocity distribution among microchannels became more uniform with larger E in this case.

However, more uniform velocity distribution could not be always achieved with larger E. It depended on the variation amplitude of pressure drops due to the changes of frictional resistances in microchannels and approximate rectangular channels of manifolds. Here a special case was illustrated in Table 3 to indicate that the value of $\sigma_U\%$ firstly decreased from 1.557 to 0.086 and then increased from 0.086 to 3.221 when E increased from 100 to 1000 μm. That was, the velocity distribution firstly became more uniform and then became non-uniform with the increase of E.

3.2. Effects of synchronous variation of microchannel width and depth

It was unrealistic to unlimitedly increase the microchannel length for obtaining relatively uniform velocity distribution due to the limited space in a given sheet. Therefore, by changing the microchannel width and depth was the most feasible method for enabling narrow velocity distribution. As described before, it indicated that the velocity distribution became more uniform with smaller W_c or larger E. However, synchronous variation of W_c and E should be considered in the realistic design process. The variations of R_{fc} due to the synchronous changes of W_c and E could be worked out by Eq. (3), as shown in Fig. 4. When W_c and E varied from 100 to 500 μm, R_{fc} could reach the minimum value when they were both equal to 500 μm, whereas the maximum value of R_{fc} could be obtained when they were both equal to 100 μm.

However, it was difficult to determine the trend of pressure drop distribution only from the variation of R_{fc} since the values of $R_{fi}(j)$ and $R_{fo}(j)$ in the inlet and outlet manifold were also changed with E. Therefore, the amplitude of variation in R_{fc} should be compared with that in $R_{fi}(j)$ and $R_{fo}(j)$. The variation of E could result in the same trends of frictional resistances of the inlet and outlet manifolds due to their centrosymmetry with each other. Here take the inlet manifold as example, and use the average value R_{fi} (m) of $R_{fi}(j)$ to represent the variations of frictional resistances of inlet manifold. And an estimating parameter K_R was defined as below to compare the variation amplitude of R_{fc} with R_{fi} (m).

$$R_{fi}(m) = \frac{1}{N}\sum_{j=1}^{N} R_{fi}(j) \tag{14}$$

$$K_R = \frac{R_{fc}}{R_{fi}(m)} \tag{15}$$

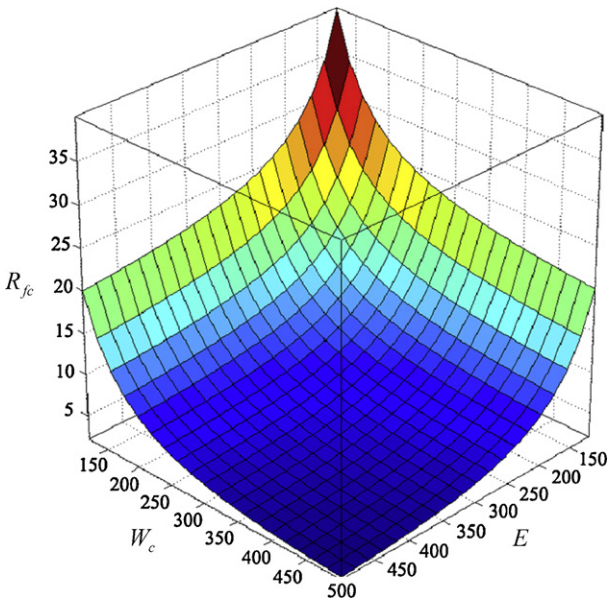

Fig. 4. Variations of R_{fc} due to the synchronous changes of W_c and E.

Table 3
A special case for the variations of σ_U% with E.

Microchannel structural parameters	$N=5$, $L_c=5$mm, $W_c=500$ μm				
Inlet manifold structural parameters	$L_m=5$ mm, $H_{in}=0.2$ mm, $X_{pi}=-1$ mm, $Y_{pi}=2$ mm, $R_{pi}=0.5$ mm				
E(μm)	100	300	500	800	1000
γ_m	0.124	0.138	0.154	2.635	3.221
$\Delta\gamma$%	14.396	0.758	11.316	24.246	29.757
σ_U%	1.557	0.086	1.226	2.635	3.221

Table 4
Variations of several estimate parameters with the synchronous changes of W_c and E.

W_c(μm)	300	250	200	150	150
E(μm)	300	350	400	450	500
R_{fc}	6.350	6.860	8.853	13.722	27.844
R_{fi}(m)	0.110	0.082	0.063	0.050	0.041
K_R	57.591	84.035	140.545	273.573	680.001
γ_m	0.814	0.882	0.937	0.973	0.977
$\Delta\gamma$%	4.475	2.849	1.659	0.933	0.833
σ_U%	1.310	0.801	0.464	0.279	0.251

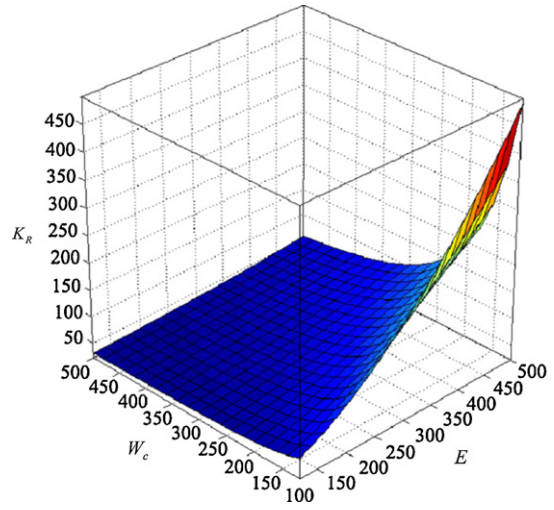

Fig. 5. Variations of K_R with the synchronous changes of W_c and E.

Fig. 5 presents how the synchronous variations of W_c and E affected the value of K_R. It indicated that K_R increased with the decreasing W_c and increasing E. The maximum value of K_R could be obtained when W_c and E were equal to 100 and 500 μm, respectively. The proportion of pressure drop in microchannels to the overall pressure drop increased with the increasing K_R, and hence led to a relatively uniform velocity distribution.

Table 4 provided special data to illustrate the variations of several estimated parameters with the synchronous changes of W_c and E. It indicated that K_R increased with smaller W_c and larger E due to the increase of R_{fc} and decrease of R_{fi} (m). The ratio of pressure drop in the microchannels to the overall pressure drop increased and led to the increase of γ_m. The value of σ_U% decreased as a result of the decrease of $\Delta\gamma$%. Therefore, high-aspect-ratio (smaller W_c and larger E) microchannels were in favor of obtaining relatively uniform velocity distribution.

3.3. Effects of manifold structural parameters

Table 5 shows how the manifold structural parameters affected the values of γ_m, $\Delta\gamma$% and σ_U%. The values of γ_m were larger than 0.64 for all the structural parameters considered here, which indicated that the pressure drops in microchannels were in the dominant position of the overall pressure drop. By comparing Table 5 with Table 2, it could be found that the amplitude of $\Delta\gamma$% varied much larger with the variation of microchannel structural parameters than that with the variation of manifold structural parameters. It indicated that the microchannel structural param-

Table 5
Effects of manifold structural parameters on the values of γ_m, $\Delta\gamma$% and σ_U%.

X_{pi}/X_{po} (mm)	−4	−2	−1	0	2
γ_m	0.686	0.721	0.743	0.768	0.824
$\Delta\gamma$%	8.064	6.710	5.961	5.186	3.686
σ_U%	2.559	2.097	1.844	1.586	1.092
Y_{pi}/Y_{po} (mm)	5	6	7	8	10
γ_m	0.651	0.690	0.721	0.747	0.787
$\Delta\gamma$%	10.147	8.136	6.710	5.658	4.236
σ_U%	3.291	2.590	2.097	1.738	1.261
L_m (mm)	14	16	20	22	30
γ_m	0.778	0.758	0.721	0.704	0.642
$\Delta\gamma$%	5.018	5.590	6.710	7.261	9.416
σ_U%	1.571	1.747	2.097	2.270	2.955
R_{pi}/R_{po} (mm)	0.5	1	2	2.5	
γ_m	0.722	0.723	0.721	0.719	0.716
$\Delta\gamma$%	7.190	6.953	6.710	6.712	6.804
σ_U%	2.328	2.236	2.097	2.050	2.023
H_{in}/H_{out} (mm)	1	2	3	4	5
γ_m	0.705	0.721	0.734	0.745	0.755
$\Delta\gamma$%	4.275	6.710	7.850	8.447	8.764
σ_U%	1.318	2.097	2.460	2.646	2.740

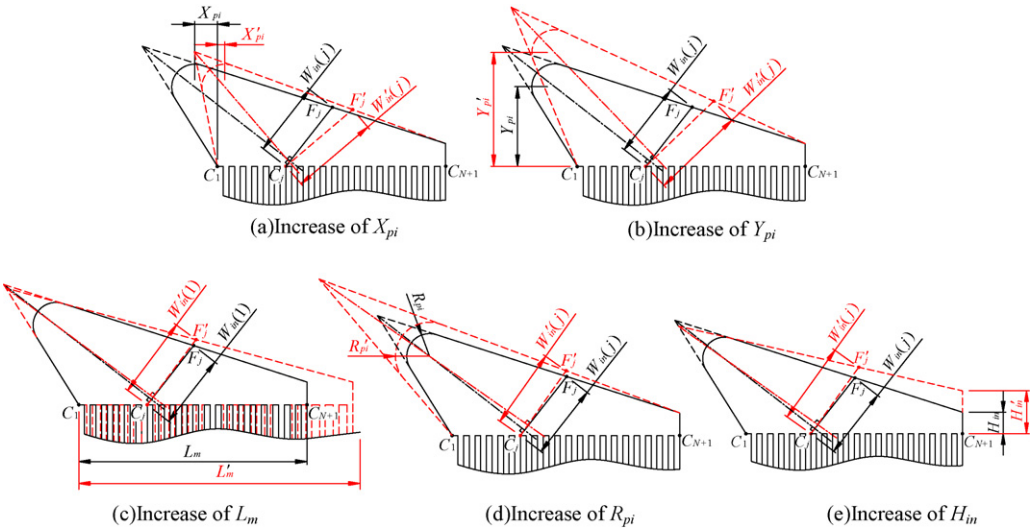

Fig. 6. Effects of manifold structural parameters on the shape of approximate rectangular channels.

eters showed more influence on the velocity distribution than that of manifold structural parameters. In other words, the velocity distribution was firstly determined by the microchannel structural parameters.

Here take inlet manifold as example, the changes of frictional resistances of approximate rectangular channels of manifolds were investigated to analyze the effects of manifold structural parameters on the pressure drop and velocity distribution among microchannels. Since the width $W_{in}(j)$ of each approximate rectangular channel was always larger than its depth E, the frictional resistance of each approximate rectangular channel could be obtained by substituting Eq. (1) into Eq. (3), as defined below:

$$R_{fi}(j) = \frac{12\,\mu}{NE^2} \frac{L_m \sin \angle F_j C_j C_{N+1}}{(1 - 0.351(E/W_{in}(j)))^2} \quad (j = 1, 2, \ldots, N) \tag{16}$$

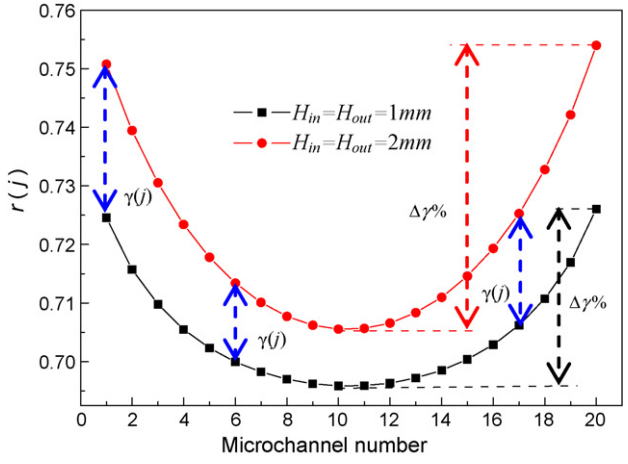

Fig. 7. Variation amplitude of $\gamma(j)$ and $\Delta\gamma\%$ when *Hin*/*Hout* changed from 1 to 2 mm.

It could be found that the frictional resistance of each approximate rectangular channel was determined by $\angle F_j C_j C_{N+1}$, $W_{in}(j)$ and L_m when the manifold structural parameters changed. By combining with descriptive geometry, the effects of manifold structural parameters on the shape of approximate rectangular channels were investigated, as shown in Fig. 6.

As shown in Fig. 6(a) and (b), $\angle F_j C_j C_{N+1}$ decreased and $W_{in}(j)$ increased with the increasing X_{pi} and Y_{pi}, which led to the decrease of $R_{fi}(j)$ according to Eq. (16). As a result, the pressure drops in inlet manifolds decreased and led to the increase of γ_m. As shown in Table 5, γ_m increased with the increasing X_{pi}/X_{po} (means X_{pi} or X_{po}) or Y_{pi}/Y_{po} (means Y_{pi} or Y_{po}). $\Delta\gamma\%$ decreased as a result of the increase of the proportion of pressure drops in microchannels, and hence the value of $\sigma_U\%$ became smaller with larger X_{pi}/X_{po} or Y_{pi}/Y_{po}.

On the other hand, both $\angle F_j C_j C_{N+1}$ and $W_{in}(j)$ increased with the increasing L_m, R_{pi} or H_{in}, as shown in Fig. 6(c–e). However, it could not be determined the trend of $R_{fi}(j)$ simply by Eq. (16). Here the value of R_{fi} (m) was used to analyze the trend of $R_{fi}(j)$. Table 6 presents the trend of R_{fi} (m) changed with L_m, R_{pi} or H_{in} for this case. It indicated that R_{fi} (m) increased with the increasing L_m. As a result, the pressure drops in inlet and outlet manifold due to frictional losses increased and the value of γ_m decreased, leading to the corresponding increase of $\Delta\gamma\%$ and $\sigma_U\%$, as indicated in Table 5.

Table 6 indicated that the changes of R_{pi}/R_{po} (means R_{pi} or R_{po}) and H_{in}/H_{out} (means H_{in} or H_{out}) showed little effects on the values of R_{fi} (m). As a result, the values of γ_m varied in a small range with the variation of R_{pi}/R_{po} and H_{in}/H_{out}. As for the variation of R_{pi}/R_{po}, the values of $\Delta\gamma\%$ also varied as a result of the fluctuation of γ_m. But $\sigma_U\%$ decreased with the increasing R_{pi}/R_{po}. The total flow increased due to the invariance of entrance velocity in this work. And the velocity value in each microchannel with smaller equivalent diameter increased more than that in the approximate rectangular channels. As a result, the pressure drops in microchannels increased and led to a relatively uniform velocity distribution.

Table 6
Variations of *Rfi* (m) with the changes of L_m, R_{pi} or H_{in}.

L_m (mm)	14	16	20	22	30
R_{fi} (m)	0.028	0.032	0.041	0.045	0.063
R_{pi} (mm)	0.5	1	2	2.5	3
R_{fi} (m)	0.039	0.039	0.0410	0.041	0.042
H_{in} (mm)	1	2	3	4	5
R_{fi} (m)	0.041	0.041	0.041	0.041	0.042

On the other hand, the values of $\Delta\gamma\%$ and $\sigma_U\%$ increased with the increasing H_{in}/H_{out}. It indicated that the increase of γ_m did not necessarily result in the decrease of $\Delta\gamma\%$. The possible reason was the variation amplitude of $\gamma(j)$ was smaller than that of $\Delta\gamma\%$. Fig. 7 shows the comparison of variation amplitude of $\gamma(j)$ and $\Delta\gamma\%$ when H_{in}/H_{out} changed from 1 to 2 mm.

4. Conclusions

Based on the previously developed model, the velocity distribution in the microchannel array with centrosymmetric triangle manifolds was analyzed in this work. And the effects of structural parameters on the velocity distribution were studied and the relationship between frictional resistances and pressure drop were investigated. It was found that the velocity distribution among microchannels became more uniform with larger L_c, E, X_{pi}/X_{po}, Y_{pi}/Y_{po}, R_{pi}/R_{po} and smaller L_m, W_c or H_{in}/H_{out}. Compared with the manifold structural parameters, the microchannel structural parameters showed more influence on the velocity distribution. High-aspect-ratio microchannels were in favor of obtaining relatively uniform velocity distribution.

From the analyses of the relationship among the frictional resistances, pressure drop and velocity distribution, it indicated that the variation of pressure drop distribution among microchannels due to the variation of frictional resistances was the underlying reason for the variation of velocity distribution among microchannels. By the combination of the calculation of frictional resistances with descriptive geometry, it could predict the trend of velocity distribution among microchannels with the variation of structural parameters by analyzing the variation trend of frictional resistances. The prediction method was useful to the design for microchannel plates with centrosymmetric triangle manifolds.

Acknowledgments

This research was supported by the National Nature Science Foundation of China, Project Nos. 50805052 and 50930005, the Fundamental Research Funds for the Central Universities, SCUT, Project Nos. 2009ZM0134 and 2009ZM0066, Shenzhen Science and Technology Program, Project No. JC200903120092A.

References

[1] P.M. Martin, D.W. Matson, W.D. Bennett, D.C. Stewart, Y. Lin, Laser micromachined and laminated icrofluidic components for miniaturized thermal, chemical and biological systems, vol. 3680, in: SPIE Conference Proceedings, Design, Test and Micro-fabrication of MEMS and MOEMS, 1999, pp. 826–833.
[2] D.W. Matson, P.M. Martin, D.C. Stewart, A.L.Y. Tonkovich, M. White, J.L. Zilka, G.L. Roberts, Fabrication of microchannel chemical reactors using a metal lamination process, in: Proceedings of 3rd International Conference on Microreaction Technology, Berlin, 2000, pp. 62–71.
[3] P.M. Martin, D.W. Matson, W.D. Bennett, D.C. Stewart, C.C. Bonham, Laminated ceramic microfluidic components for microreactor applications, in: AIChE 2000 Apring National Meeting, Atlanta, 2000.
[4] J.M. Commenge, L. Falk, J.P. Corriou, M. Matlosz, Optimal design for flow uniformity in microchannel reactors, AIChE Journal 48 (2002) 345–357.
[5] C. Amador, A. Gavriilidis, P. Angeli, Flow distribution in different microreactor scale-out geometries and the effect of manufacturing tolerances and channel blockage, Chemical Engineering Journal 101 (2004) 379–390.
[6] O. Tonomura, S. Tanaka, M. Noda, M. Kano, S. Hasebe, I. Hashimoto, CFD-based optimal design of manifold in plate-fin microdevices, Chemical Engineering Journal 101 (2004) 397–402.
[7] E.R. Delsman, A. Pierik, M.H.J.M. De Croon, G.J. Kramer, J.C. Schouten, Microchannel plate geometry optimization for even flow distribution at high flow rates, Chemical Engineering Research and Design 82 (A2) (2004) 267–273.
[8] M. Pan, Y. Tang, H. Yu, H. Chen, Modeling of velocity distribution among microchannels with triangle manifolds, AIChE Journal 55 (8) (2009) 1969–1982.